

DEVELOPMENT OF INPUT COUPLER FOR COMPACT ERL MAIN LINAC

Hiroshi Sakai[#], Takaaki Furuya, Masato Sato, Kenji Shinoe, Kensei Umemori,
KEK, Tsukuba, Ibaraki, 305-0801, Japan

Masaru Sawamura, JAEA, Tokai, Naka, Ibaraki, 319-1195, Japan

Enrico Cenni, The Graduate University for Advanced Studies, Tsukuba, Ibaraki, 305-0801, Japan

Abstract

We fabricated the prototype of an input coupler, which has two ceramic windows to keep the inside of the superconducting cavity clean, for ERL main linac and performed the high power test. Required input power is about 20kW with standing wave condition for the cavity acceleration field of 20MV/m. In this high power test, the one ceramic window, named as a cold window, was installed into the vacuum insulating chamber and cooled by liquid Nitrogen. First, the multipacting at 10kW level prevented the power increasing. By using the pulse processing method for 8 hours, power finally reached the 25kW with standing wave condition. We could also keep feeding 20kW power into coupler for 16 hours. From these results of high power test, this prototype coupler satisfied our thermal and RF requirements. In this paper, we present the recent results about the prototype of input coupler.

INTRODUCTION

An input coupler is one of the important items of the superconducting cavity for ERL operation [1]. Table 1 shows the parameters of the input coupler for main linac. Though the mechanism of energy recovery enables to reduce the input power of the main linac, the minimum input power will be restricted by the cavity detuning due to the microphonics from a cryomodule. Therefore, 20kW is needed for our main linac operation.

Table 1: Parameters of Input Coupler for Main Linac

Frequency	1.3GHz
Accelerating voltage	Max 20MV/m
Input power	Max CW 20kW (Standing wave)
Loaded Q (Q_L)	$1 \times 10^7 \sim 4 \times 10^7$ (variable)

Figure 1 shows the design of the input coupler for our main linac. Two coaxial disk ceramic windows are set; One, which is called as “cold window”, is set on the cold parts at 80K and the other, which is called as “warm window”, is on warm parts at 300K for safety against vacuum leak due to window break. Purity of ceramic material is 99.7% to reduce the power loss of ceramic. The impedance of coupler is 60Ω to reduce the power dissipation of inner conductor. Furthermore forced air cooling was applied to inner conductor. Detailed design strategy and parameters are expressed in Ref.[2].

[#] sakai.hiroshi@kek.jp

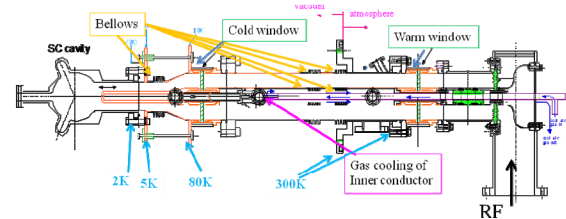


Figure 1: Schematic design of input coupler for main linac.

Previously, we fabricated input coupler components, warm ceramic windows with bellows and cold windows, and carried out the high-power test of the components by using a CW 30kW IOT power source. In these component tests, we found the resonance of the dipole mode in ceramic window made the sudden temperature rise and the break of ceramic window [3][4]. We fabricated the new ceramic window by changing the thickness of ceramic window to escape the resonance mode. We finally achieved 27kW in the high power test by using new ceramic window [5]. The high power test of the components of input coupler was successfully carried out. Therefore, we fabricated a prototype of input coupler of ERL main linac (TOSHIBA TETD). In this proceeding, we summarized the following results of prototype input coupler. First the high power test of input coupler was carried out under Liq. N₂ cooling. We also carried out the thermal-cycle tests of cold ceramic window by using this input coupler again. The low level test was also carried out by using ERL 9-cell cavity.

HIGH POWER TEST OF THE PROTOTYPE OF AN INPUT COUPLER UNDER LIQUID NITROGEN COOLING

According to the components test with the high power test and the thermal cycle test, we slightly changed the parameters of ceramic window. We fabricated the first prototype of input coupler as shown in the left figure of Fig. 2. Fig. 3 shows the setup of high power test of input coupler with standing wave. RF power was fed into the input coupler from 30kW IOT via a doorknob exchangers and reflected by the end plate. The standing wave was excited, however, not to stand the peak field at the bellows and ceramic windows in high power test as shown in the right figure of Fig. 2. Especially we'd like to know the real temperature rises under vacuum insulation as same as the cryomodule by feeding the high power, the

input coupler was inserted into the vacuum insulator and the cold window was cooled by the liquid nitrogen tank via the 4 copper braid lines whose length was 200mm and total cross section was 400mm². The cold window was surrounded by the Al cold box connected with liquid nitrogen tank to reduce thermal radiation between the cold window and the outside set on the room temperature. Other coupler components set into the vacuum insulator were also surrounded by super insulators with the enough thickness. Many temperature sensors were set to mainly monitor the temperatures of bellows and warm/cold window as shown in Fig. 3.

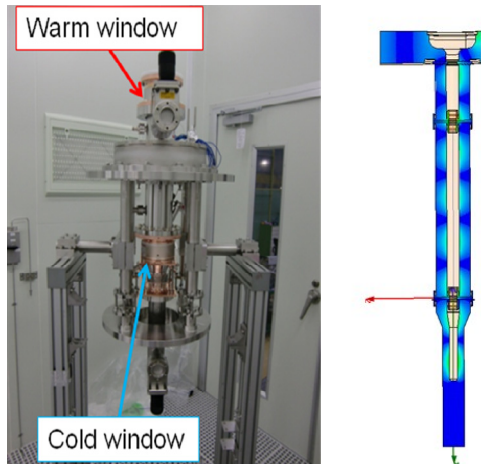


Figure 2: (Left) Picture of the prototype of the input coupler for ERL main linac. (Right) Simulation of magnetic field distribution of input coupler at test stand.

Forward RF power (P_{in_for}) and reflected RF power (P_{in_ref}) were also measured at the upstream of the doorknob exchanger. The inner conductor and bellows were cooled via rod by N₂ gas from the cold evaporator and the amount of gas flow was monitored. The flow of N₂ gas was usually kept 115 l/min in this test. Two arc sensors were set; one was on the end plate to see the cold window (arc1), the other was on the outer conductor near the warm window (arc2). The volume between the cold window and the end plate (light blue area in the lower figure of Fig. 3) and the volume between two ceramic window (green area in the lower figure of Fig. 3) were separately pumped by each ion pump and the vacuum pressures were measured by each CCG (named as CCG1 on light blue area and CCG2 on green area), respectively. After baking over 150 °C for 24 hours, the vacuum pressures of 1.5x10⁻⁶ Pa of CCG1 and 7x10⁻⁷ Pa of CCG2 were achieved before high power test, respectively. Three electron probes (e-probe 1-3) were also set near the ceramic windows to detect the secondary electrons under processing as shown in the lower figure of Fig.3.

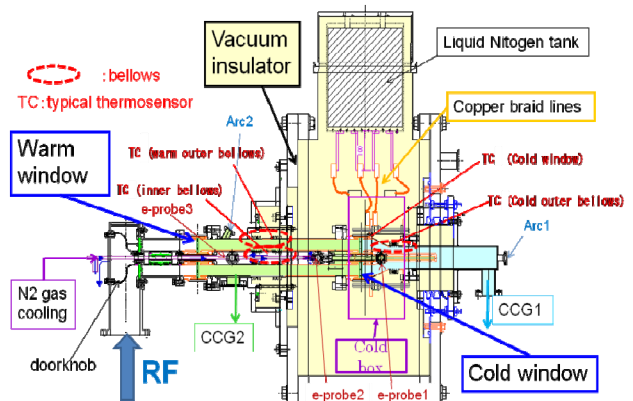
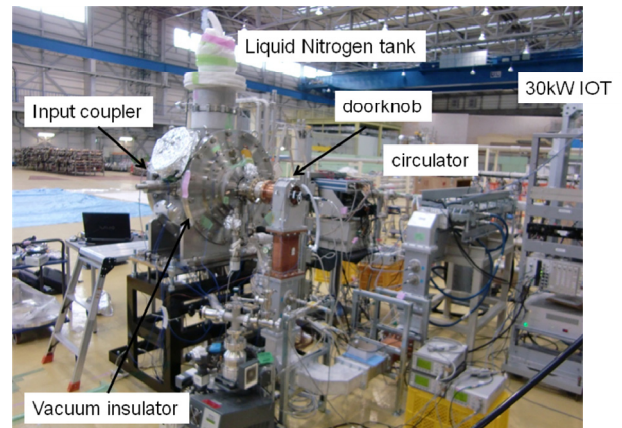


Figure 3: (upper) Picture of the setup of high power test of the input coupler under liquid nitrogen cooling. (lower) The detail of the setup of the high power test including the inside of the vacuum insulator.

We applied the RF power to this input coupler. First we could smoothly increase the RF power until 20kW. At 20kW, suddenly arc (arc2) and vacuum (CCG2) interlocks worked. Unfortunately, feeding power was down to 10kW and could not overcome 10kW level under CW power feeding. Fig. 4 shows the signal detected by electron probe set near the warm window (e-probe3). Whenever the arc interlock (arc1) worked, the vacuum of warm window increased and the e-probe signal was detected. Since the processing for one hour with same method, failed to increase the feeding power, could not be increased, we tried the pulse processing with 30μs pulse width.

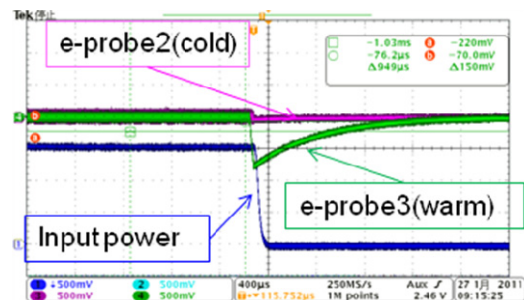


Figure 4: Signals come from electron probe (e-pick3) when the arc interlock was occurred.

Figure 5 shows the processing history up to 25kW. After searching the optimum processing condition of the pulse processing, feeding power gradually increased under keeping the lower vacuum pressure than 1×10^{-4} Pa for 8 hours. The vacuum of warm window (CCG2) and electron probe of warm window (e-probe3) indicated that the processing activated the area between two ceramics and finally we reached the 25kW power level. After changing to the CW power feeding at 25kW as shown in Fig. 5, the vacuum pressure of cold window (CCG1) slightly increased. The both vacuum pressures, however, gradually decreased under keeping the 25kW level. This shows the processing was in progress and finally we could not detect the secondary electron by electron probes. The processing was smoothly carried out by using the pulse processing.

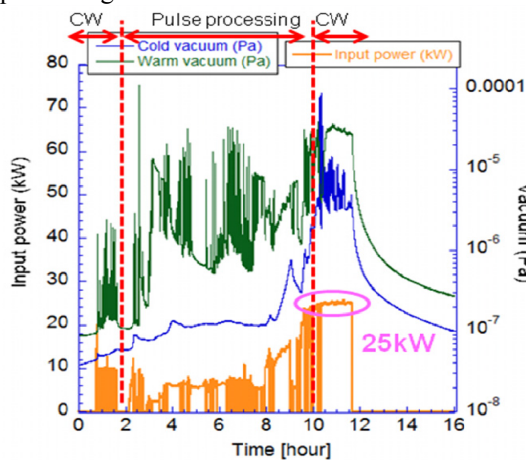


Figure 5: History of the power processing up to 25kW. The left vertical axis shows the input power (P_{in}) (orange). The right vertical axis shows the vacuum pressure (CCG1:blue & CCG2:green). Red array shows the region of different condition of processing.

Next we kept the power at 20kW level in order to measure the temperature rise under the liquid nitrogen cooling with the vacuum insulator. Fig. 6 shows the history of the power, vacuum pressure (upper) and the temperatures (lower) whose measured positions were drawn in the lower figure of Fig. 6, by keeping 20kW standing wave to the input coupler. The power of 20kW was kept for 16 hours to become the equilibrium condition of the measured temperature. During the stable power feeding, arc interlocks worked three times. These interlocks came not from the electron activity inside the input coupler but from the unknown electrical noise of arc sensors. Furthermore, vacuum pressure increased once unless the interlock worked. This was because the lack of the liquid nitrogen in the tank. Therefore, we fed the liquid N_2 to the tank soon and keep the temperature stable again. In the upper figure of Fig. 6, first the vacuum pressures increased up to 4×10^{-6} Pa of CCG1 and 1×10^{-6} Pa of CCG2. After 8 hours from 20 kW power feeding, the vacuum pressures were decreased as the temperature

reached the equilibrium condition. We stopped power feeding after 16 hours later when the temperature was stable. The maximum temperature of 127 °C was measured at the inner conductor bellows. This temperature rise of inner conductor bellows was not so high that the vacuum would not be wrong and reasonable value compared with other experiment like Ref.[6]. We were anxious about the temperature rise (ΔT) of outer conductor bellows near warm window, which is shown by the black line in the lower figure of Fig. 9, to increase much higher. However, we noted that the temperature rise of 70K was not so high in spite of setting this bellows inside the vacuum insulator, compared with other experiment in Ref[7]. This is, I think, because 150 μ m thick plating of the half of the warm bellows was applied and the much heat load in the bellows would transfer outside. This copper plating worked effectively.

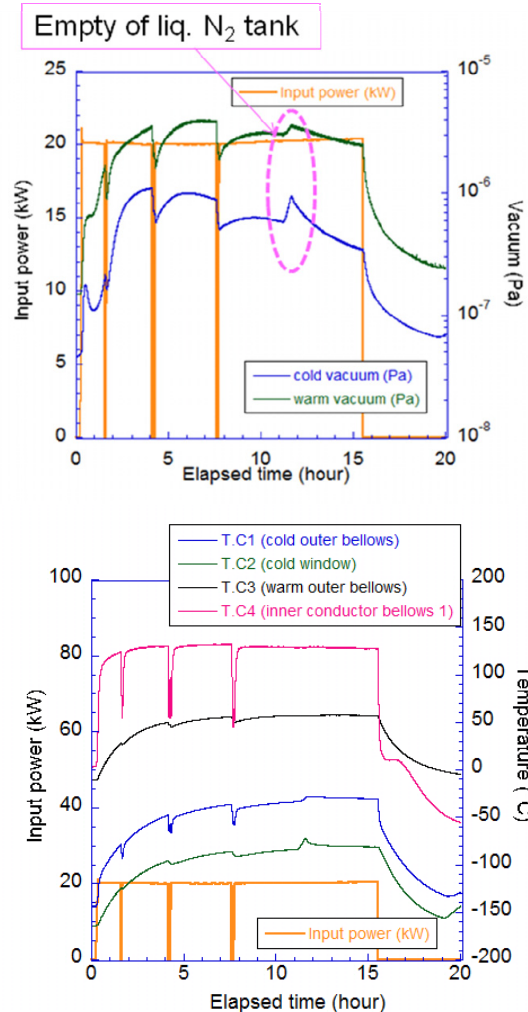


Figure 6: The history under keeping 20kW input power. (upper) The input power (orange) vs vacuum pressure (CCG1:blue & CCG2:green). (lower) The input power (orange) vs temperature rise. Blue (green, black, pink) shows the temperature at cold outer bellows (cold window, warm outer bellows, inner conductor bellows).

The temperature rise of cold window and outer bellows near cold window were 100K, which was also reasonable value. Roughly calculated heat load of the cold window from the temperature measurements of braid lines was twice bigger than expected. One reason was the poor vacuum pressure of the vacuum insulator of 3×10^0 Pa. The cold window might be not perfectly isolated thermally from the outside.

In order to check the memory effect by processing, we warmed up the input coupler to the room temperature and exposed the inside of the input coupler to the air for 4 hours. After cooling the coupler again by liquid nitrogen with vacuum insulator, we noted that we could smoothly increase up to 24kW power level again. We did not detect the arc interlock or secondary electron by electron probes, under feeding power up to 24kW again.

THERMAL CYCLE TESTS OF COLD CERAMIC WINDOW OF PROTOTYPE INPUT COUPLER

Previously, we carried out the thermal cycle test between 80K and room temperature by using the old cold window prior to the fabrication of the prototype of the input coupler of main linac. The cold window was gradually cooled by filling up a cooler box with evaporating N_2 gas for several hours and finally reached to 80K. After keeping 80K for a few hours, the cold window was warmed up for half and/or a day and we carried out the leak check. After the fifth thermal cycle test, the leak ratio of ceramic window drastically increased from 1×10^{-10} Pa m^3/s to 1×10^{-4} Pa m^3/s . We thought that the ceramic window was broken under thermal cycle tests. After the color-check of the ceramic window to identify the leak point, we found the leak point at inner conductor as shown in Fig.7. To see the leak point precisely, we cut the ceramic window and inspected the cross section in detail. There appeared the red color line of the cross section of the ceramic window as shown in Fig.7. This broken line like the arch was typically explained by the thermal stress test under brazing between the different materials with different thermal conductivities like ceramic and metal in Ref.[8]. The thermal-stress analysis by ANSYS also explained that the edge of the ceramic window near the inner conductor have the biggest thermal stress. We continued the simulation of ANSYS to reduce the thermal stress by changing the parameters of inner copper support thickness and inner support of molybdenum thickness and length. Decreasing the thickness of copper and increasing the thickness of molybdenum mainly enabled to reduce the thermal-stress down to 78% from the original value. According to these results, we changed the brazing condition to newly calculated parameters and applied these conditions for fabrication of prototype of input coupler.

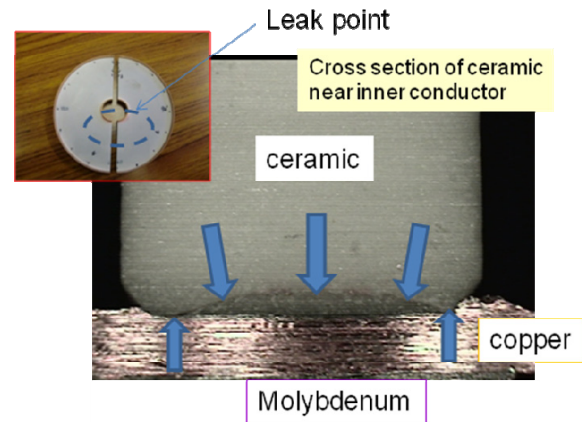


Figure 7: The pictures of ceramic window (left) and the cross section of ceramic window (center). The red arch line with blue arrows shows the broken line of the ceramic.

After high power test of prototype input coupler, we continue the liquid nitrogen cooling of the cold window by using same setup in order to carry out the thermal cycle test; we emphasized that the blazing condition of this cold window of input coupler was modified from old one. Fig. 8 shows the temperature change of cold window from the 3rd to the 10th thermal cycle test. The cold window was gradually cooled down for several hours and warmed up for more than half day not to add the sudden thermal shock to the ceramic. After the 10th thermal cycle test, we could not detect the leakage over 1×10^{-10} Pa m^3/s by a He leak detector. By changing the blazing condition of cold window, we found that the cold window could stand 10-times thermal cycle from liquid N_2 to the room temperature. Furthermore, we found that no leaks or damages of ceramic windows and bellows were observed after this high power test.

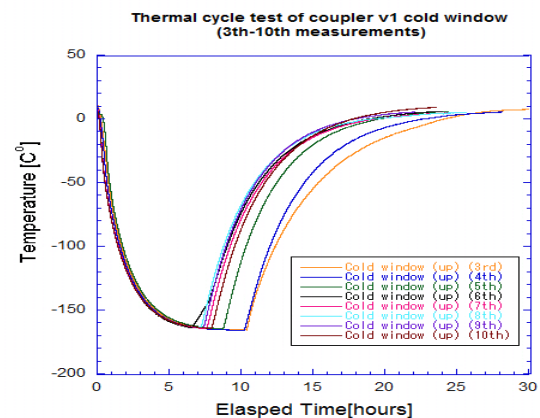


Figure 8: The temperature data from 3rd to 10th thermal cycle test. 1st and 2nd thermal cycle test were done under the high power test.

MEASUREMENT OF COUPLING OF PROTOTYPE INPUT COUPLER

By using prototype input coupler and ERL 9cell cavity, we measured the Q_{ext} of input coupler directly as shown in Fig.9. Q_{ext} was measured by changing the distance from the cavity center. We note that we measured the coupling with doorknob exchanger.

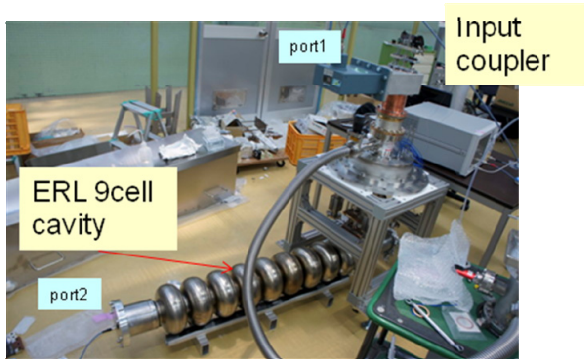


Figure 9: Measurement setup of Q_{ext} of input coupler with doorknob exchanger.

Figure 10 shows the measurement results of Q_{ext} change by changing the distance from the cavity center comparing with the calculation values of HFSS and MW-Studio[9]. Slope of Q_{ext} change with coupler length agree well with calculation. However the measured value of Q_{ext} with doorknob exchanger is 1.3 times lower than calculation. Prior to the fabrication of two input couplers for cERL cryomodule, we will change the length of 2mm shorter by using the measurement results.

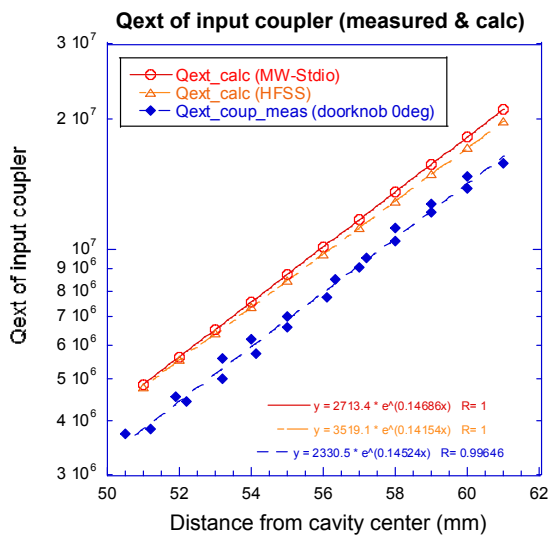


Figure 10: Q_{ext} change by changing the distance from the cavity center. Red and orange plots shows the calculation by MW-Studio (red) and HFSS (orange). Blue solid circles show the coupling measurement results by using prototype coupler with doorknob exchanger.

SUMMARY

Prior to the fabrication of the prototype of the input coupler, we carried out the thermal cycle test of the old cold window between liquid nitrogen and room temperature. After the 5th thermal cycle test, the ceramic window near the inner conductor was cracked. This phenomenon was almost agreed well with the calculation by simulation and we applied the new brazing parameters, which reduced the thermal stress based on simulation, to the new prototype of input coupler. Next, we carried out the high power test of this input coupler under liquid nitrogen cooling with the vacuum insulator. After pulse processing for 8 hours, we finally achieved 25kW with standing wave in the high power test. By keeping 20kW input power for 16 hours, we also measured the temperature rise. The maximum temperature rise was measured at the bellows of the inner conductor. However, the temperature rise was suppressed down to 120K by N₂ gas cooling of 115 l/min flow. The vacuum pressure was also suppressed at $\sim 10^{-6}$ Pa under 20kW power feeding. We noted that we could smoothly increase up to 24kW power level again after warming up to room temperature and exposing the inside of the input coupler to the air for 4 hours. In addition, after the high power test, we continued the liquid nitrogen cooling of the cold window by using the same setup in order to carry out the thermal cycle test. By changing the brazing condition of the cold window, we could increase the thermal cycles up to 10 times and no crack or leak was observed after these tests. The coupling measurement was also done by using ERL-9cell cavity directly. These values also agreed well with the expected values.

The thermal and RF power tests were successfully done with the prototype of input coupler and the basic design of the input coupler has satisfied our requirements by these tests. In this year, we will fabricate the two input couplers for the main linac to prepare the compact ERL construction.

ACKNOWLEDGEMENT

We thank the KEK RF Group, especially T. Miura, for preparing the RF source and the KEK Cryogenic group, especially Y. Kojima for preparing the liquid nitrogen evaporator. We also thank K. Onoe from University of Tokyo for helping the measurement of the thermal cycle test of the cold window.

REFERENCE

- [1] S. Sakanaka, et.,al, "Status of the energy recovery linac project in Japan", PAC'09, Vancouver, May (2009).
- [2] H. Sakai et al., "Development of a 1.3GHz 9-cell superconducting cavity for the Energy Recovery Linac", Proceedings of ERL07 Workshop, Daresbury, (2007).

- [3] H.Sakai et al., “Development of input power coupler for ERL main linac in Japan”, Proceedings of 14-th SRF Workshop, Berlin, (2009).
- [4] K.Umemori et al, “Observation of Resonance mode in coaxial-type input coupler”, Proceedings of IPAC2010, Kyoto, (2010).
- [5] H.Sakai et al, “Power coupler development for ERL main linac in Japan”, Proceedings of IPAC2010, Kyoto, (2010).
- [6] W.Anders et al., “CW operation of superconducting TESLA cavities”, Proceedings of 13-th SRF Workshop, Beijing, (2007).
- [7] V.Veshcherevich et al, “High Power Tests of input couplers for Cornell ERL injector”, Proceedings of 13-th SRF Workshop, Beijing, (2007).
- [8] K.Suganuma et al, “Joining of ceramics and metals”, Ann. Rev. Mater. Sci. 1988, 18: p47-73 (1988).
- [9] T.Muto et al., “The calculation of transverse kick by the input coupler of superconducting cavity for ERL main linac”, Proceedings of the 7th Annual Meeting of Particle Accelerator Society of Japan , p840-842 (THPS024), Himeji, Japan.